JOURNAL OF MATERIALS SCIENCE 28 (1993) 795–798

Preparation and crystallization of Fe–Co–B amorphous powder

F.-S. LI, D.-S. XUE
Department of Physics, Lanzhou University, Lanzhou 730000, People's Republic of China

Ultrafine $(Fe_{0.7}Co_{0.3})_{100-x}B_x$ amorphous powders with boron content x in the range 27–40 at % have been prepared by borohydride reduction. The preparation process shows that the powders have a catalysis property. The results of X-ray and electron diffractions show that all of the samples were spherical amorphous particles of dimension < 0.2 µm. The difference in the ease of composition between Fe–Co–B powder and ribbon indicates that the local environment of Fe–Co–B powder may be different from that of Fe–Co–B ribbon. The study of crystallization behaviour using Mössbauer, X-ray and differential scanning calorimetry measurements indicates that there are two steps in the crystallization process. These steps represent the formation of α-$Fe_{70}Co_{30}$ phase and Fe_2B-like phase, respectively.

1. Introduction

Recently the preparation of amorphous powder by borohydride reduction has attracted increasing attention [1–5] as the amorphous powder can be prepared at room temperature, which is much lower than the melting point, T_m, and glass transition point, T_g, of the amorphous alloy. This means that the formation mechanism of amorphous powder is different from that of amorphous ribbon obtained by rapid quenching, and one might ask if there is any difference between Fe–Co–B amorphous powder and ribbon. In this paper we report the preparation technology of Fe–Co–B amorphous powders with a wide range of composition and the characteristics of the crystallization behaviour of the powders.

2. Experimental procedure

First, aqueous solutions of $NaBH_4$ (or KBH_4) and a mixture of $FeSO_4 \cdot 7H_2O$ and $CoCl_2 \cdot 6H_2O$ were made in a certain volume and concentration, respectively. Then the solution of above divalent metal salt was dropped smoothly into the solution of reducing agent BH_4^- with vigorous stirring. The black precipitate was washed with deionized water, ethanol and acetone in that order after filtration, then dried with a cold air flow. If the reaction conditions are appropriate, the black precipitate will be Fe–Co–B amorphous powder.

The boron content in the samples was analysed by the acid–base volume method. The structure and morphology of the specimens were measured using a D/MAX-3A X-ray diffractometer with a K_α radiation of Fe, and EM-400T transmission electron microscopy. Thermal stability of the samples was measured using a CDR-1 type differential dynamic calorimeter. Mössbauer spectra were recorded using a FH1913 conventional constant acceleration spectrometer at room temperature. A 10 mCi ^{57}Co (Rh) source was used.

3. Results and discussion

The amorphous powders of $(Fe_{0.7}Co_{0.3})_{100-x}B_x$ were prepared using a method similar to that reported elsewhere [4]. The results and technological factors are shown in Table 1. From Table 1, it is seen that the amorphous powder with boron content of around 40 at % can be prepared easily at room temperature. If an amorphous powder with lower boron content is required, the following measures should be taken:

1. Decrease the reaction temperature.
2. Decrease the pH value of solution.
3. Apply an external magnetic field.

However, the pure amorphous powder with B content around 20 at % is difficult to obtain even by taking a series of special measures. On the other hand, the Fe–Co–B amorphous ribbon with B content around 20 at % can easily be made by the rapid quenching technique, but the ribbon with higher B content cannot be made conventionally. This difference may result from the different short range order (SRO) which results in a significant difference of boron content between the powder and ribbon. This result agrees with that of the Fe–B amorphous powder reported in Ref. 5.

When KBH_4 (40 ml and 2 mol) reacted with divalent metal salt (20 ml and 0.5 mol) at 7 °C, the precipitate often ignited naturally in the drying process. The Mössbauer spectrum of ignited precipitate was given in Fig. 1. It is found that the sample is crystallized fully and no oxide phase exists in it. According to the differential scanning calorimetry (DSC) results given below, the ignition temperature is higher than 700 K. This means that the powder has a catalysis property. The following results also reflect this property:

TABLE I Technological conditions for the preparation and the boron content in the precipitate (CA:citric acid, LA:lactic acid)

KBH_4 concentration (mol)	$NaBH_4$ concentration (mol)	$Fe^{2+} + Co^{2+}$ (+ Acid)		Reaction temperature (°C)	Boron content in sample (at %)
		Volume (ml)	Concentration (mol)		
1		100	0.1	19	40
1		100	0.09	6	37
	0.5	100	0.09	6	33
1		100	0.1 (+ 0.02CA)	6	30
	0.25	100	0.05 (+ 0.02CA)	6	27
	0.25	100	0.05 (+ 0.069LA)	6	24
	0.25	20	0.25 (+ 0.03CA)	6	21
	0.25	20	0.25 (+ 0.1CA)	6	18

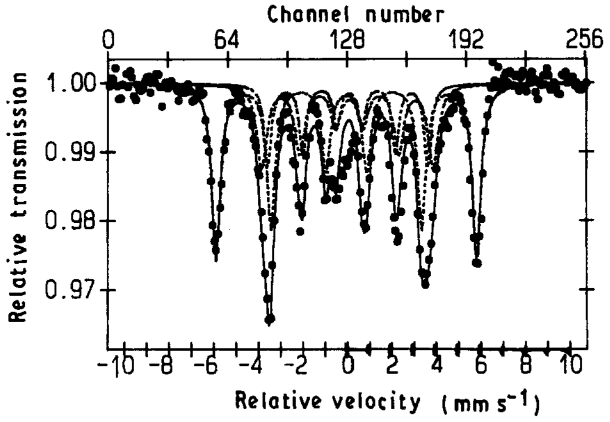

Figure 1 Mössbauer spectrum of ignited sample at room temperature.

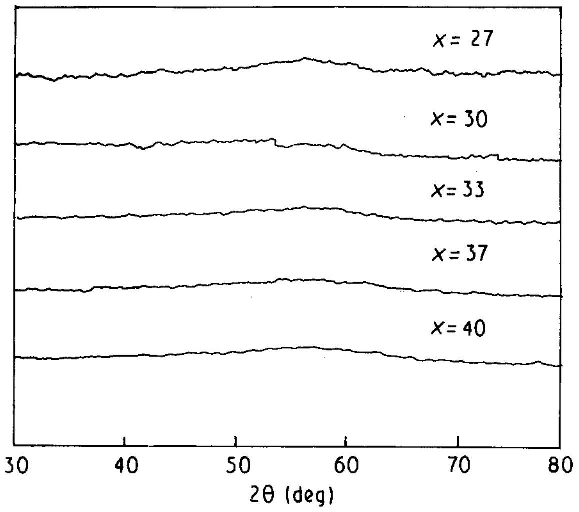

Figure 2 X-ray diffraction patterns of $(Fe_{0.7}Co_{0.3})_{100-x}B_x$ amorphous powders at room temperature.

1. In the reduction process, it is found that a vigorous reaction appeared as soon as the precipitate formed.

2. If the dried amorphous powder was taken into a new fresh BH_4^- solution, the hydrolysis reaction became stronger. This may be the reason why the divalent ions were used in the preparation process of H_2 with BH_4^- [6].

Fig. 2 shows the X-ray diffraction patterns of Fe–Co–B amorphous powders measured at 30 kV and 30 mA. The diffraction profiles indicate that there is only one typical broad pattern of amorphous structure and no crystalline peaks, as X-ray diffraction is not sensitive enough to distinguish the microcrystals from the ultrafine amorphous powder. All the samples were measured with transmission electron microscopy to exclude the possibility of the existence of small microcrystal particles and to view the morphology of amorphous powders. As an example, Fig. 3a shows the electron diffraction pattern and Fig. 3b shows the morphology of $(Fe_{0.7}Co_{0.3})_{63}B_{37}$. It is found that most of the particles are regular spheres with diameter less than 0.2 μm. The typical amorphous ring shown in Fig. 3a confirms the amorphous state of the samples. Thus the transmission electron microscopy (TEM) results indicate that the specimens with B content in the range 27–40 at % were spherical amorphous particles. If the B content in the precipitate is less than 27 at %, there is often a certain amount of α-$Fe_{70}Co_{30}$ in the precipitate.

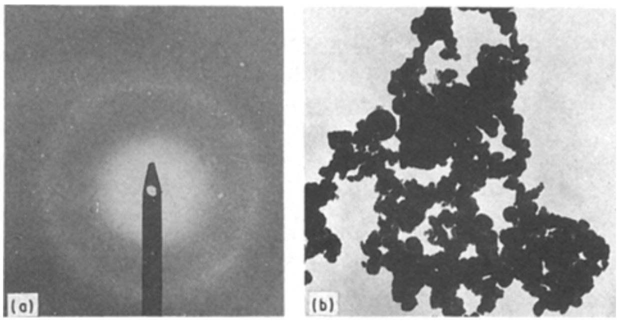

Figure 3 (a) electron diffraction pattern and (b) Spherical morphology of $(Fe_{0.7}Co_{0.3})_{63}B_{37}$ at room temperature.

Under argon atmosphere, DSC curves of the specimens were measured with a rate of temperature increase of 20 K min^{-1}. It is found that there are two exothermal peaks in the curves which appear at increasing temperature with increasing B content. This result indicates that these peaks represent two steps of the crystallization process and the greater the content of B in the powder, the higher the thermal stability of the powder. From X-ray results, the first peak indicates that an α-Fe-like phase formed, and the second peak results from the appearance of a Fe_2B-like phase [3]. Fig. 4 shows the X-ray diffraction pattern of

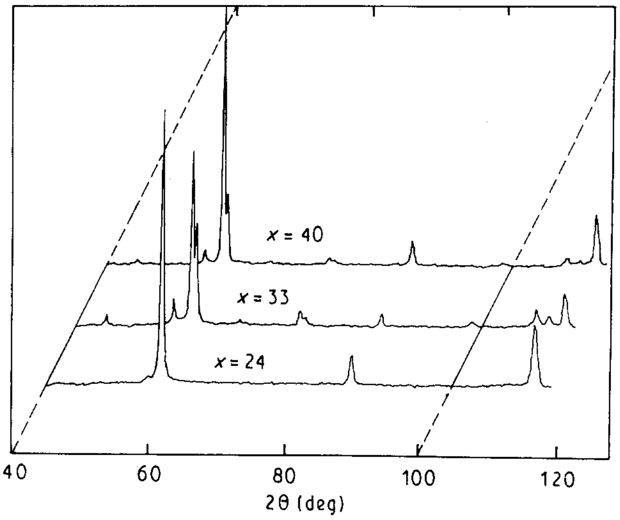

Figure 4 X-ray diffraction patterns of crystallized $(Fe_{0.7}Co_{0.3})_{100-x}B_x$ ($x = 24, 33, 40$) samples at room temperature.

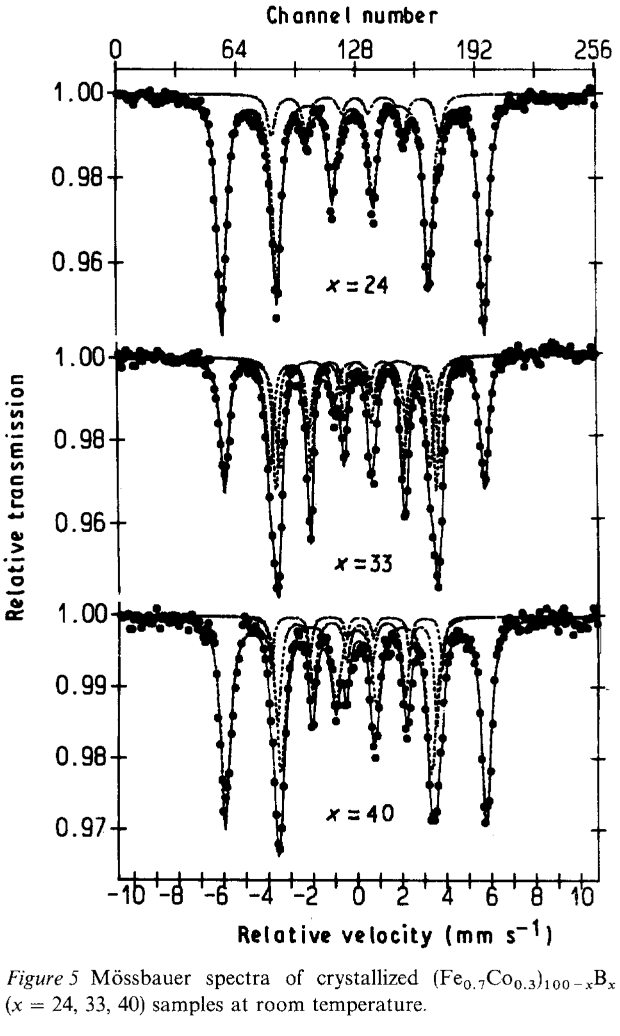

Figure 5 Mössbauer spectra of crystallized $(Fe_{0.7}Co_{0.3})_{100-x}B_x$ ($x = 24, 33, 40$) samples at room temperature.

crystallized $(Fe_{0.7}Co_{0.3})_{100-x}B_x$ ($x = 24, 33, 40$) samples. It is not clear, however, where the Co atoms go.

TABLE II The fitting results of crystallized $(Fe_{0.7}Co_{0.3})_{100-x}B_x$ ($x = 24, 33, 40$) sample, isomer shift (IS) is relative to α-Fe

x	Crystallization phase	Content (%)	Hyperfine field, H_{hf} (T)	IS (mm s^{-1})
24	$Fe_{70}Co_{30}$	86	36.5	0.03
	Fe_2B	14	23.7	0.12
33	$Fe_{70}Co_{30}$	68	36.6	0.03
	Fe_2B	8	24.0	0.12
	$(Fe\text{–}Co)_2B_x$	24	22.4	0.13
37	$Fe_{70}Co_{30}$	42	36.4	0.03
	Fe_2B	30	23.9	0.12
	$(Fe\text{–}Co)_2B$	27	22.4	0.13

The Mössbauer spectra of these crystallized samples, shown in Fig. 5, indicate that there are two or three phases in the crystallized products. Its fitting results are shown in Table 2. For the lower boron content powder $(Fe_{0.7}Co_{0.3})_{78}B_{24}$, it is found that α-$Fe_{70}Co_{30}$ alloy with a hyperfine field (HF) of 36.4 T [7] appeared at first which results from the nucleation and the growth of the α-$Fe_{70}Co_{30}$ microcrystalline phase. Then a Fe_2B phase which has a 23.9 T HF [8] formed. For the higher boron content power, an α-$Fe_{70}Co_{30}$ alloy also appeared first in the crystallization process. Then the Fe_2B phase and the $(Fe\text{–}Co)_2B$ [8] phase (HF = 22.5 T) formed at the same time. From the crystallization products and its composition, the possibility of the existence of other cobalt and boron compounds cannot be excluded.

4. Conclusions

(a) Adjusting the technological factors, ultrafine $(Fe_{0.7}Co_{0.3})_{100-x}B_x$ ($27 \leqslant x \leqslant 40$) amorphous powders can be prepared in a wide range of B content. The size of spherical powders is smaller than 0.2 μm.

(b) The ultrafine particles of Fe–Co–B have a catalysis property.

(c) Replacing 30 at % Fe atoms with Co atoms, the higher boron content Fe–Co–B amorphous powder can easily be made at room temperature. In contrast, the amorphous ribbons with higher boron content cannot. This means that the formation process of amorphous powder is quite different from that of ribbons. The SRO of the powder may be different from ribbon of the same composition.

(d) The crystallization of $(Fe_{0.7}Co_{0.3})_{100-x}B_x$ ($x = 24, 33, 40$) indicates that there are two steps of the crystallization process of the powders. The α-$Fe_{70}Co_{30}$ phase appeared first. Then Fe_2B or Fe_2B and $(Fe\text{–}Co)_2B$ phases formed. The temperature at which each phase appeared increased with increasing B content.

Acknowledgements

The authors are grateful to Professor Y. D. Zhang and Professor D. Li for useful discussions. This work is partially supported by the National Natural Foundation of China.

References

1. J. van WONTERGHEM, S. MORUP, C. J. W. KOCH, S. W. CHARLES and S. WELLS, *Nature* **322** (1986) 622.
2. L. D. DRAGIEVA, M. S. SLAVCHEVA and D. T. BUCHKOV, *J. Less-Common Metals* **117** (1986) 311.

3. A. CORRIAS, G. ENNAS, G. LICHERI, G. MARONGIU, A. MUSINU, G. PASCHINA, G. PICCALUGA, G. PINNA and M. MAGINI, *J. Mater. Sci. Lett.* **7** (1987) 407.
4. D. S. XUE, F. S. LI and R. J. ZHOU, *J. Mater. Sci. Lett.* **9** (1990) 506.
5. F. S. LI, D. S. XUE and R. J. ZHOU, *Hyperfine Interactions. Int.* **55** (1990) 1021.
6. H. I. SCHLESINGER, H. C. BROWN, A. E. FINHOLT, J. R. GILBREATH, H. R. HOEKSTRA and E. K. HYDE, *J. Amer. Chem. Soc.* **75** (1953) 215.
7. K. SUMIYAMA and Y. NAKAMURA, *Phys. Stat. Sol.* **105** (a) (1988) 291.
8. L. TAKACS, M. C. CADEVILLE and I. VINCZE, *J. Phys.* **F5** (1975) 800.

Received 18 November 1991
and accepted 7 January 1992